



**A Wearable Microfluidic Device Integrated with
a Sensor and Potentiostat for Sweat Sodium
Monitoring**

by

**Nur Fatin Adini binti Ibrahim
(2231313670)**

A thesis submitted in fulfillment of the requirements for the degree of
Master of Science (Biomedical Electronic Engineering)

**Faculty of Electronic Engineering & Technology
UNIVERSITI MALAYSIA PERLIS**

2024

PERMISSION TO USE

In presenting this thesis in fulfillment of the requirements for a postgraduate degree from Universiti Malaysia Perlis (UniMAP), I agree that permission for the copying of this thesis in any manner, in whole or in part, for scholarly purpose may be granted by the Director of the Centre for Graduate Studies. It is understood that any copying or publication or use of this thesis or parts thereof for financial gain shall not be allowed without my written permission. It is also understood that due recognition shall be given to me and to Universiti Malaysia Perlis (UniMAP) for any scholarly use which may be made of any material from my thesis.

Requests for permission to copy or to make other use of materials in this thesis, in whole or in part, should be addressed to:

Director, Centre for Graduate Studies
Administration Block, 1st Floor,
Engineering Training Center Building,
Pauh Putra Campus, 02600 Arau Perlis
Tel : +604-9885712 Fax : +604-9885740,
e-mail : cgs@unimap.edu.my

ACKNOWLEDGEMENT

In the name of Allah, the Most Gracious and the Most Merciful, Alhamdulillah. I express my deepest gratitude to Almighty God, Allah s.w.t, for His will, grace, and love that have eased my journey in completing my research works on this study topic.

Special appreciation goes to my supervisor, Dr. Anas Mohd Noor, for his supervision, and expert advice from the beginning until the completion of this research project. I heartily acknowledge his invaluable constructive comments, suggestions, and patience throughout the experimental, journal writing, and thesis works. His guidance has shown me the right path whenever I faced any problem in this study, and his contributions have undoubtedly contributed to the success of this research work. I am also truly fortunate to have Dr. Norhayati Sabani as my co-supervisor. Her dedication to guidance and providing insights into the experimental method is truly commendable. She never fails to impress me with her valuable comments and priceless knowledge related to my research experiments. Moreover, her encouragement and moral support contribute significantly to boosting my confidence when I feel uncertain. In addition, I am indeed blessed to have both of you because you also provide all the equipment and the best facilities to ease my work, which I have benefited from.

I would like to express my sincere appreciation to Mr. Muhammad Emi Azmel Shohini for his technical support, sharing his expertise and skills, and providing facilities during the development of the microfluidic device and We-VoltamoStat. Additionally, I would like to thank the Universiti Malaysia Perlis laboratory staff for their assistance during my time in the laboratory. I also extend my heartfelt thanks to the unnamed subject who willingly volunteered to participate in my research project.

I would like to extend my utmost appreciation and heartfelt gratitude to my beloved parents, Ibrahim Yusoff and Faridah Che Salam, and lovely family for their unwavering support, continuous prayers, love, and motivational words. Their encouragement has been instrumental in pushing me to go the 'extra mile' and has been a source of strength whenever I am lost or stuck in the project. I also want to express my sincere thanks to my dear friends for their concern, understanding, and moral support.

All their presence has been a pillar of my strength, helping me face the challenges along this journey. I am truly grateful for each one of you. Thank you from the bottom of my heart for being there for me. May Almighty Allah continue to bless, abundantly reward, and protect each of you.

TABLE OF CONTENTS

	PAGE
DECLARATION OF THESIS	i
PERMISSION TO USE	ii
ACKNOWLEDGEMENT	iii
TABLE OF CONTENTS	iv
LIST OF TABLES	vii
LIST OF FIGURES	ix
LIST OF ABBREVIATIONS	xiv
LIST OF SYMBOLS	xv
ABSTRAK	xvi
ABSTRACT	xvii
CHAPTER 1 : INTRODUCTION	1
1.1 Research Background	1
1.2 Problem Statements	4
1.3 Research Objectives	6
1.4 Research Hypotheses	6
1.5 Research Scopes	7
CHAPTER 2 : LITERATURE REVIEW	9
2.1 Introduction	9
2.2 Fundamental of a Sweat-Sensing System	9
2.2.1 Sweat Compositions	9

2.2.2	Sweat Rate	12
2.2.3	Sodium Ion Detection Process in Sweat	14
2.3	Liquid Flow Control Approach	15
2.4	Bonding Method	21
2.4.1	Irreversible Bonding	21
2.4.2	Reversible Method	22
2.5	Fabrication of Microfluidic Device	26
2.6	Hydrophilic and Hydrophobic Materials	32
2.7	Measurement Techniques	35
2.8	Recent Developments in Potentiostat	42
2.9	Conclusion	48
CHAPTER 3 : METHODOLOGY		50
3.1	Introduction	50
3.2	Block Diagram Fabrication and Testing for Wearable Sweat Sodium Sensing	50
3.3	Preparation of Artificial Sweat	51
3.4	Microfluidic Device	54
3.4.1	3D Model Design	56
3.4.2	Slicing of 3D Model	60
3.4.3	Printing Microfluidic Device	61
3.4.4	Post-Processing	62
3.4.5	3D Printing Parameters Tuning	62
3.4.6	Microfluidic Chip Flow Test	65
3.4.7	Assembly	66
3.5	Sensor	67
3.6	Developed Potentiostat	68
3.6.1	Design and Development the We-VoltamoStat	69

3.6.2	Calibration and Validation Method of the We-VoltamoStat	70
3.6.2.1	Calibration of We-VoltamoStat	71
3.6.2.2	Sodium Analysis Method	76
3.7	Real-Time Monitoring	80
3.8	Conclusion	81
CHAPTER 4 : RESULTS & DISCUSSION		83
4.1	Introduction	83
4.2	Microfluidic Chip Flow Performance	83
4.3	We-VoltamoStat Performance	85
4.3.1	Calibration Test Performance	85
4.3.2	Accuracy Test of Custom Mode Measurements	88
4.3.3	Validation of the We-VoltamoStat including Accuracy, Selectivity and Stability	96
4.4	Real-Time Monitoring	104
4.5	Conclusion	106
CHAPTER 5 : CONCLUSION		108
5.1	Conclusion	108
5.2	Future Works	110
REFERENCES		111
LIST OF PUBLICATIONS		130

LIST OF TABLES

	PAGE
Table 2.1 Summary of printed microfluidic devices using VPP technology.....	30
Table 2.2 The EIS measurement includes capacitance and interface resistance.....	36
Table 2.3 Summary of previous works on development potentiostat.....	46
Table 3.1 Required mass of powder and volume of distilled water for preparing stock solution of NaCl, KCl and CaCl ₂	52
Table 3.2 Volume of stock solution and distilled water required for preparing 10 mL NaCl, KCl, and CaCl ₂ samples ranging from 10 to 200 mM.....	54
Table 3.3 Optimal print settings of the developed microfluidic chip and sensor holder.....	65
Table 3.4 The input parameters settings for three measurement modes using a bare SPE.....	77
Table 4.1 Result for test of printed microfluidic device performance.....	84
Table 4.2 The average current reading between the Keithley device and the potentiostat.....	87
Table 4.3 The percentage error in measuring the current and the average current in LSV measurements, using Metrohm and We-VoltamoStat, for NaCl solutions with concentrations of 10mM, 50mM, and 100mM.....	94
Table 4.4 Sensor output for NaCl concentration ranging from 1 – 250 mM for Metrohm instrument and We-VoltamoStat.....	98

Table 4.5	Validation of We-VoltamoStat through paired sample t-test with Metrohm instrument for sodium analysis.....	100
Table 4.6	Tukey test analysis for sensor currents ranging from 10-200mM between the target ion and interference ions using We-VoltamoStat.....	103
Table 4.7	Measurement of sweat sodium levels in terms of current and concentration, expressed in mM and ppm, at 10, 20, and 30 min	106

©This item is protected by original copyright

LIST OF FIGURES

		PAGE
Figure 1.1	Wearable sweat sensing device	4
Figure 2.1	Analysis of sweat sensing applications (Ibrahim et al., 2022).....	11
Figure 2.2	Human body maps of absolute regional median sweat rates during exercise (Smith & Havenith, 2011).....	14
Figure 2.3	Sodium ion measurements process.....	15
Figure 2.4	Conventional methods for sweat collection use sweat-absorbing materials, including (a) paper (Jain et al., 2019), (b) sponge (Huang et al., 2014), (c) nanotextile disks in wearable epidermal patches (K. Zhang et al., 2021), and (d) textiles in regular outfits (Wicaksono et al., 2020).	16
Figure 2.5	Types of fluid flow control approaches for microfluidic devices	17
Figure 2.6	The fluid flow control approach within a microfluidic device such as (a) capillary effect (Wei et al., 2022), (b) gravity effect (Y. Yang et al., 2019), (c) absorption-based paper (Liang et al., 2021), (d) finger actuation (Reeder et al., 2019), (e) active pump using the piezo-electric sound (Conde et al., 2015), (f) iontophoresis (Sempionatto & Gao, 2022), (g) microneedle injection with transdermal drug delivery (Parrilla et al., 2022), and (h) valve (He et al., 2023).....	18
Figure 2.7	The methods for reversible mechanical clamping in microfluidic devices, including (a) screw and nut, (b) screw only, (c) hinge and hole-connector, (d) hinge and stopper, (e) hinge aligner, (f) magnet, and (g) magnet arrangements in gasket and PDMS	25

Figure 2.8	Fabrication techniques of microfluidic device.....	26
Figure 2.9	Natural micropump within microchannel with a few factors considered such as (a) hydrophilic and hydrophobic surfaces (Baghban, 2018), (b) graph of treated and untreated hydrophobic surfaces (Tian et al., 2018), and (c) position flow rate with surface distribution (Giorello et al., 2020).	33
Figure 2.10	Example of an EIS graph with a Nyquist plot (Ghosh et al., 2017).....	35
Figure 2.11	Example of potentiometry graphs: (a) open-circuit potential responses, plotted as voltage against the logarithm of sodium ion concentration, and (b) calibration curve (Jalal et al., 2024.....	37
Figure 2.12	Example of amperometry graph (Jaworska et al., 2019).....	39
Figure 2.13	The CV curves of SPE/ChPBN with arrows indicate an increase in scan rate from 10 to 100 mV/s, a process used to measure sodium ion levels (Ghosh et al., 2017).....	40
Figure 2.14	Example of a LSV graph (G. Hussain & Silvester, 2018).....	41
Figure 2.15	Recent developments in potentiostat design, featuring (a) flexible thin-layer PCB substrates for wearability (Criscuolo et al., 2021), (b) integration of colorimetric sensing for visual detection (Alam et al., 2023), and (c) real-time measurement of multiple specified analytes (M. Hu et al., 2024).	43
Figure 3.1	The block diagram of the process flow for developing a wearable sweat sodium sensing.....	51
Figure 3.2	The wearable microfluidic device and potentiostat integrate with a sodium sensor	55
Figure 3.3	Fabrication and testing of printed microfluidic device.....	56

Figure 3.4	The 3D model design of microfluidic chip showing (a) front view, (b) back view, and (c) side view.	57
Figure 3.5	Microfluidic chip dimensions.....	58
Figure 3.6	The 3D model design of sensor holder with (a) opening and closing lid, (b) dimensions, and (c) assembly of the microfluidic chip and sensor holder with a sodium sensor, ready for wearability.....	59
Figure 3.7	Default setting for standard rigid resin clear for 0.05 mm.....	60
Figure 3.8	Steps for printing the sliced 3D model	61
Figure 3.9	Post-processing of printed microfluidic device.....	62
Figure 3.10	Printed microfluidic device using default settings showing (a) 1 mm outlet with the closed channel diminished, (b) micropillars added to a 1.5 mm outlet closed channel at three different heights, (c) open channel at the outlet with dimensions of 0.05, 0.3, and 0.5 mm, and (d) redesigned sensor holder to prevent elephant foot deformation.	63
Figure 3.11	Illustration of sweat fully filling the sensor channel and beginning to flow out at the external outlet.	66
Figure 3.12	The printed microfluidic device with (a) separated parts of the microfluidic chip and sensor holder, (b) assembly of the microfluidic chip and sensor holder, (c) assembly of both parts with a few accessory components, and (d) wearing the device on the arm.....	67
Figure 3.13	The types of sensors used are: (a) bare SPE and (b) sodium sensor.	68
Figure 3.14	Functional block diagram of We-VoltamoStat	69
Figure 3.15	Validation method for the We-VoltamoStat	71

Figure 3.16	The configuration setup for the resistor test includes (a) the SMD resistors board and (b) its connection setup with the We-VoltamoStat.....	73
Figure 3.17	The current measurement of the potentiostat has been tested using a Keithley instrument.	74
Figure 3.18	The dummy cell tests were conducted using (a) the Metrohm instrument and (b) the We-VoltamoStat, both with a scan rate of 25 mV/s.....	75
Figure 3.19	Configuration setups for two different sensors. The setup for a SPE is connected to (a) the Metrohm instrument and (b) the We-Voltamostat.....	76
Figure 3.20	The setup for a sodium sensor is connected to (a) the Metrohm instrument and (b) the We-Voltamostat.....	78
Figure 3.21	The wearable devices for a wireless sweat-sensing system.....	81
Figure 4.1	Contact angle on the surface of water washable resin and conventional resin.....	83
Figure 4.2	Accuracy test result (a) voltage source, (b) nano-ampere test, (c) micro-ampere test, and (d) milli-ampere test.....	86
Figure 4.3	The results from both tests are plotted for comparison.	88
Figure 4.4	CV analysis of bare SPE with Metrohm instrument and We-VoltamoStat: 10 mM NaCl, 0.1-0.5 V/s scan rate.....	90
Figure 4.5	CV analysis of bare SPE with Metrohm instrument and We-VoltamoStat: 50 mM NaCl, 0.1-0.5 V/s scan rate.....	91
Figure 4.6	CV analysis of bare SPE with Metrohm instrument and We-VoltamoStat: 100 mM NaCl, 0.1-0.5 V/s scan rate.....	92
Figure 4.7	LSV analysis of bare SPE with Metrohm instrument and We-VoltamoStat: 10, 50 and 100 mM NaCl, 0.1-0.5 V/s scan rate.....	93

Figure 4.8	Amperometry measurements, using Metrohm and We-VoltamoStat, for NaCl solutions with concentrations of 10mM, 50mM, and 100mM, include a percentage error.....	95
Figure 4.9	The amperometry measurement results using a sodium sensor with Metrohm and We-VoltamoStat, comparing concentrations of (a) 10 mM, (b) 50 mM, (c) 100 mM, (d) 150 mM, and (e) 200 mM of NaCl.....	97
Figure 4.10	The Bland-Altman plots for concentration ranging of 1-250 mM.....	99
Figure 4.11	Figure 4.9 Amperometry results show average current plots for (a) sensor respond, (b) concentration range of 10-200 mM, and (c) concentration range of 1-250 mM.....	101
Figure 4.12	Selectivity test results in graphical analysis for target in the presence of the interference ions.....	102
Figure 4.13	The results of the sweat sodium measurement include the following graphs: (a) continuous current and concentration within 30 minutes and (b) average current and concentration at 10-minute intervals up to 30 minutes.....	105

LIST OF ABBREVIATIONS

ADC	Analog-Digital Converter
App	Application
Au/CNT	Gold-Carbon Nanotube
Au/CNT/Au	Gold-Carbon Nanotube-Gold
CHG	Charger
ChPBN	Chitosan Prussian Blue Nanocomposite
CAD	Computer-Aided Design
CNC	Computer Numerical Control
FDM	Fused Deposition Modelling
GPIO	General Purpose Input/Output
ISE	Ion-Selective Electrode
IPA	Isopropyl Alcohol
LCD	Liquid Crystal Display
LSV	Linear Sweep Voltammetry
PB	Prussian Blue
PDMS	Polydimethylsiloxane
PEDOT(Cl)	Poly(3,4-ethylenedioxythiophene) Chloride
PEDOT(PSS)	Poly(3,4-ethylenedioxythiophene) Polystyrene Sulfonate
PEGDA	Poly (ethylene glycol) diacrylate
PG	Power Ground
PMMA	Poly (methyl methacrylate)
RSR	Regional Sweat Rate
SLA	Stereolithography
SMC	Surface Mount Component
SPDT	Single-Pole Double-Throw
SPE	Screen-Printed Electrode
SSD	Sweat Sensing Device
TET	Terephthalate
TIA	Transimpedance Amplifier
TS	Terminal Stand
WP	Wiper
VPP	Vat photopolymerization

LIST OF SYMBOLS

A	Area
$CaCl_2$	Calcium Chloride
C_b	The bulk concentration of electroactive species
D	Diffusion coefficient
F	Faraday's constant
I	Current
KCl	Potassium chloride
M_{sample}	Molarity of the sample solution
$M_{\text{stock solution}}$	Molarity of the stock solution
n	Number of electrons involved in the reaction
Q	Surface over time
Q_{dl}	Double-layer charge
$V_{\text{distilled water}}$	Volumes of distilled water
V_{sample}	Volume of the sample solution
$V_{\text{stock solution}}$	Volume of the stock solution

©This item is protected by original copyright

Peranti Mikrobendalir Boleh Pakai yang Digabungkan dengan Sensor dan Potensiostat untuk Pemantauan Natrium dalam Peluh

ABSTRAK

Peranti sensor boleh pakai, termasuk untuk aplikasi pemantauan peluh manusia, kini mendapat perhatian untuk tujuan bukan invasif seperti pemantauan kecergasan dan diagnosis penyakit. Namun, peranti ini menghadapi masalah berkaitan dengan kebolehpercayaan dan ketepatan data. Masalah tersebut termasuk pengumpulan jumlah sampel yang terhad, kecekapan dan aliran berterusan pengumpul sampel peluh, kebolehpercayaan sensor, serta ketepatan dan kestabilan peranti elektrokimia. Sebuah peranti mikrobendalir dengan saluran bersaiz mikro telah dihasilkan untuk meningkatkan jumlah sampel bagi mengumpul peluh yang terhad dalam julat mikroliter dan untuk mengurangkan pencemaran bendasing. Ia juga telah dioptimumkan untuk aliran peluh yang berkesan dengan menggunakan bahan yang boleh dibasuh dengan air, memberikan permukaan hidrofilik kepada peranti mikrobendalir tersebut. Peranti mikrobendalir ini direka dengan saluran menegak yang meningkatkan daya graviti untuk memudahkan aliran cecair yang berterusan, mencegah aliran balik, dan mengurangkan pencampuran kepekatan peluh lama dan baru. Potensiostat sebagai peranti pengukuran elektrokimia telah direka dengan bersaiz kecil, padat, dan ringan, sesuai untuk aplikasi boleh pakai. Peranti potensiostat ini mengukur arus elektrik dengan tepat dalam julat dari milli- hingga nanoampere apabila voltan diubah. Ujian sel dummy menunjukkan bahawa sifat elektrik adalah stabil, dengan kedua-dua potensiostat komersial dan yang dihasilkan menunjukkan bentuk lengkung yang serupa. Dalam ujian pengukuran natrium, peranti ini menunjukkan ketepatan prestasi yang tinggi, disokong oleh julat keyakinan 95% daripada analisis Bland-Altman. Variabiliti peranti dicirikan oleh koefisien variasi kurang daripada 4% dan korelasi intrakelas 0.998 dalam julat ion natrium 10 mM hingga 200 mM. Peranti ini juga menunjukkan selektiviti yang baik untuk ion natrium walaupun terdapat ion-ion pengganggu lain, dengan perbezaan min yang kecil untuk setiap kepekatan yang berbeza. Ia menunjukkan kestabilan yang baik, dengan sisihan piawai yang kecil sebanyak 7. Keputusan daripada aktiviti senaman menunjukkan penurunan tahap natrium daripada 112 nA kepada 91 nA dalam masa 10 hingga 30 minit, bersesuaian dengan kepekatan dalam julat 101 hingga 67 mM. Penurunan ini selari dengan kehilangan natrium yang dijangka dalam badan manusia dari semasa ke semasa. Kesimpulannya, peranti boleh pakai yang dicadangkan menawarkan kemampuan aliran berterusan dan pengukuran natrium peluh yang tepat, menangani cabaran utama dalam teknologi boleh pakai masa kini.

A Wearable Microfluidic Device Integrated with a Sensor and Potentiostat for Sweat Sodium Monitoring

ABSTRACT

Wearable sensing devices, including the application of human sweat monitoring, are currently gaining attention for noninvasive purposes such as fitness tracking and even disease diagnostics. However, these devices encounter challenges related to reliability and data accuracy. For instance, the challenges include the collection of limited sample volumes, the efficiency and continuous flow of the sweat sample collector, sensor reliability, and the accuracy and stability of the electrochemical device. A microfluidic device with micro-sized channels has been developed to improve sample volume for collecting limited sweat samples in the microliter range and to reduce contamination. It has also been optimized for effective sweat flow by utilizing a water-washable material, which provides the microfluidic device with a hydrophilic surface. The microfluidic device has been designed with a vertical channel that enhances gravitational force to facilitate continuous fluid flow, prevent backflow, and reduce the mixing of old and new sweat concentrations. The developed potentiostat, an electrochemical analyzer, has been designed with a compact and lightweight form factor suitable for wearable applications. This device accurately measures electrical current across a range from milli- to nanoamperes when the voltage is varied. Dummy cell tests showed that the electrical properties are stable, with both the commercial and developed potentiostats exhibiting similar curve shapes. In sodium measurement tests, the device demonstrates high-performance accuracy, supported by a 95% confidence interval from Bland-Altman analysis. Device variability is characterized by a coefficient of variation of less than 4% and an intraclass correlation of 0.998 in the 10 mM to 200 mM sodium ion range. The device also shows good selectivity for sodium ions in the presence of other interfering ions, as it shows a small mean difference for each different concentration. It exhibits good stability, with a small standard deviation of 7. The results from the exercise activity reveal a decrease in sodium levels from 112 nA to 91 nA within 10 to 30 minutes, corresponding to concentrations ranging from 101 to 67 mM. This decrease aligns with the expected loss of sodium in the human body over time. In conclusion, the proposed wearable devices offer continuous flow capabilities and accurate sweat sodium measurements, addressing key challenges in current wearable technologies.

CHAPTER 1 : INTRODUCTION

1.1 Research Background

Health assessment frequently relies on standard blood and physiologic analysis in detecting certain diseases and health conditions. However, these methods, particularly blood analysis, is an intrusive and costly procedure. This approach necessitates blood samples' extraction using a needle that causes physical trauma, pain, bruising skin, and risk of infection. Moreover, blood analysis is time-consuming, demands expensive tool (i.e., blood analyzer), and commonly involves the cost of sample management and other charges, which raises the overall cost. As a result, researchers are constantly looking for a practical alternative to replace the usage of blood samples to detect a disease in a short time, at a lower cost of operation, and suitable for real-time evaluation and continuous measurement. Interestingly, they found other possible biofluids such as tears (Pieragostino et al., 2015; Tiffany, 2003; Williams, 2005), saliva (Oncescu et al., 2013; Pfaffe et al., 2011; Segal & Wong, 2008; Stevenson et al., 2019), urine (C. K. Chen et al., 2020; Oshi et al., 2021; Shukuya, 2014) and sweat (Li et al., 2022; Yuan et al., 2019; Yue et al., 2022), which are also promising to be used for non-invasive purposes such as fitness tracking and even disease diagnostics.

However, certain biofluids, such as tears, are not suited for continuous sample collection because they might irritate the eyes and are difficult to be collected. (Rentka et al., 2017). Other such as saliva is not appropriate due to jeopardizing the data's veracity since the chemical composition of saliva relies on the food/drink taken by the individual or may be contaminated by blood due to mouth inflammation (Gardner et al., 2020). Meanwhile, urine is too smelly, contaminated, not appropriate for wearable application,

and impossible to collect for continuous monitoring due to excessive hydration (Kintz, 1996). Fortunately, sweat is more suitable to be applied for continuous monitoring and analysis without many other implications to the human subject.

Sweat analysis can be continuously tracked in real-time, quantifying sweat biomarkers and progressing towards self-monitoring without requiring specialized expertise. This effortless enhancement of proactive health management enables individuals to monitor their health conditions with lower cost, faster results, and more practicality. Furthermore, sweat is the most reliable biofluid sample, which corresponds to a high correlation in certain biomarkers' concentrations discovered in the blood, such as sodium (Bulmer & Forwell, 1956; Patterson et al., 2000), chloride (Bulmer & Forwell, 1956; Morrison, 1990), potassium (Sato, 1973, 1977; Sato et al., 1989), and ethanol (Buono, 1999; Schummer et al., 2008), relating to the accurate analysis in disease diagnosis. In addition, sweat samples can easily be obtained through both active perspiration (e.g., physical exercise) and passive perspiration (e.g., hot environments), external stimulants (e.g., iontophoresis), or other stimuli (e.g., stress, intake of hot drinks, spicy food, and alcohol).

The volume of secreted sweat per glands are typically in the microliter range. Hence, micro-collector devices are essential in biofluid measurement to gather limited samples in microliters or smaller for analysis. Sweat collection devices have been recently utilized using microfluidic devices (X. M. Chen et al., 2019; Escobedo et al., 2021; Nyein et al., 2018; Y. Zhang et al., 2020) and absorbent-based materials (Bae et al., 2019; Jain et al., 2019; Wicaksono et al., 2020). However, microfluidic devices offer several advantages over the conventional absorbent pads, particularly in terms of efficiency and practical. Microfluidic devices are designed to precisely control sweat

fluid flow at the microscale or typically in submillimetre confined, allowing for highly accurate and reproducible measurements (Fallahi et al., 2019). Additionally, the microfluidic channel can be designed to optimize the flow of sweat and minimize evaporation or contamination. Moreover, microfluidic devices can be integrated with sensors for real-time analysis of sweat biomarkers, providing instant feedback and enabling personalized health monitoring. Furthermore, a microfluidic device consisting of channels that link from inlet to outlet opening able to prevent mixing new and old sweat during measurement (Bariya et al., 2018), which contributes to the accuracy of continuous measurement (Heikenfeld, 2016).

Most of wearable sweat-sensing devices consist of three main components: a microfluidic device, a sensor, and a potentiostat, as shown in Figure 1.1. When sweat is secreted, the microfluidic device collects a sample and delivers it to the sensor. The sensor then detects a specific target analyte and converts its chemical signal into an electrical signal. Finally, the potentiostat measures the electrical signal using various techniques, such as potentiometric, amperometric, voltametric, or electronic impedance spectroscopic (EIS) measurements (Phoonsawat et al., 2022; Xu, Cheng, Yuan, et al., 2019). One of the most appealing aspects of wearable sweat sensing technology is its ability to wirelessly transmit data to a smartphone app or a cloud-based platform. This wireless transmission capability enhances the accessibility, usability, and effectiveness of the technology in various wearable applications, including healthcare, fitness tracking, and personalized health monitoring.

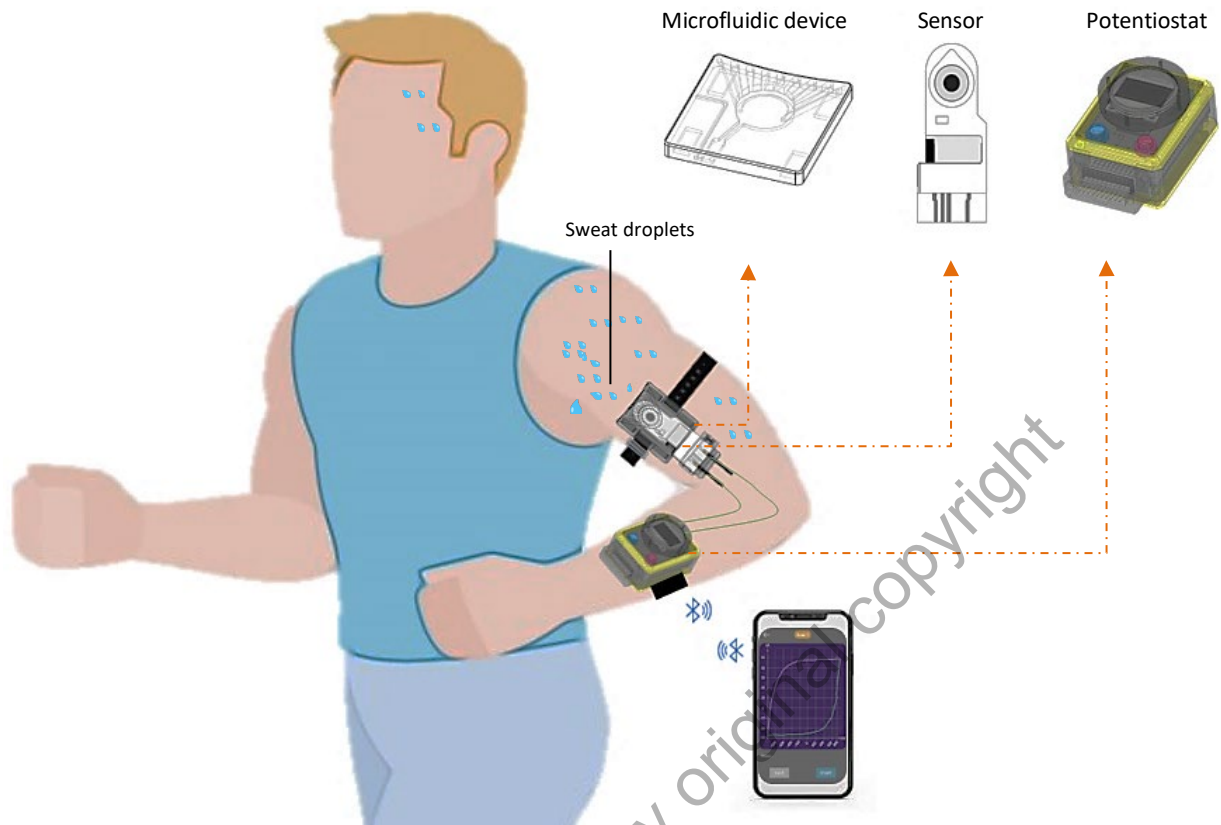


Figure 1.1 Wearable sweat sensing device

1.2 Problem Statements

Conventional sweat collection techniques, which rely on absorbent substances like filter paper (Jain et al., 2019), cotton (Bae et al., 2019), textile (Y. Yang et al., 2017), and sponge (Huang et al., 2014), have several limitations. All these substances can cause fast evaporation that reduces the sample collection, an inevitable mix of fresh and old sweat concentration, limit sweat collection based on type and thickness, and contamination. Alternative sweat collection device, such as a microfluidic device, is needed to address these issues. Despite the benefits of microfluidic devices, there are still some gaps in most designs regarding real-time measurement and continuous flow, such as the need for integration with sensors and becoming wearable devices.

Moreover, microfluidic devices integrated with electrodes can usually be used one time and hard handling maintenance, as their permanent assembly and bonding methods, such as multiple adhesive sealings (Agarwal et al., 2024). Developing reusable microfluidic devices with alternative designs is essential to reduce material waste, costs, and time spent on refabrication. Microfluidic devices are often made from hydrophobic materials, and while efforts are made to convert them into hydrophilic surfaces for better fluid flow, durability becomes a concern (Elvira et al., 2022; Preetam et al., 2022). These modified surfaces can degrade over time, reverting to hydrophobic states due to environmental factors (Nemani et al., 2018). This disrupts fluid flow in microchannels, reducing device efficiency. Choosing robust hydrophilic materials is crucial for maintaining fluid flow performance (Miao et al., 2020). Hydrophilic surfaces promote better wetting, ensuring that fluids adhere more strongly to the surface due to stronger interactions between water molecules and the surface (Fan & Guo, 2020; Wu et al., 2022).

On the other hand, many commercially available potentiostats face limitations that make these devices unsuitable for wearable applications due to high cost, bulkiness, heavy weight, and reliance on wired connections. Furthermore, these devices may have higher power consumption, limiting suitability for long-term and continuous use. These challenges highlight the need for the development of more portable, cost-effective, and user-friendly potentiostats specifically designed for wearable applications. The development of a potentiostat may concern in result uncertainty regarding its effectiveness in various aspects such as accuracy and stability. A validation process is crucial to ensure that the development potentiostat is a dependable and efficient equipment for electrochemical measurements and applications such as sensing sodium in sweat.

1.3 Research Objectives

The general objective is to develop a wearable microfluidic device and potentiostat integrated with a sensor for real-time measurement of sweat sodium, with potential applications in health monitoring. The specific research objectives are described below:

1. To fabricate a reusable and wearable microfluidic device for sweat sampling integrated with sodium sensor.
2. To develop a wearable potentiostat device for measuring and continuously collecting data on sweat sodium levels.
3. To analyze the microfluidic device for fluid flow efficiency and the potentiostat for accuracy, selectivity, and stability in sweat sodium measurements.

1.4 Research Hypotheses

The research hypotheses are discussed as below:

1. The shape, dimensions and materials of a microchannel fabrication can significantly impact fluid flow efficiency. Circular and rectangular shapes promoting laminar flow, while triangular shapes promote turbulent flow. Additionally, small channels within micrometres with hydrophilic material surfaces can promote fast fluid flow without the need for additional active pumps.
2. Combining features of wireless communication, portable battery, mini size, and lightweight design can significantly enhance the wearable potentiostat's functionality, making it user-friendly tool across different applications.

3. If the sensor currents measured by the developed potentiostat closely align with those of commercially potentiostat, the developed potentiostat can be considered reliable and accurate.
4. If the measured currents of the analyte for specific concentrations in a solution are distributed closely or on the calibration plot, it demonstrates the presence of the target analyte, indicating high selectivity. Outlier points of measured current show that the analyte is not the target analyte.
5. If low standard deviation and standard error mean, indicating high stability and precision.

1.5 Research Scopes

The research scopes are discussed as below:

1. The design of the microfluidic device should address concerns such as ensuring that channel dimensions at the outlet are smaller than 1mm to reduce fluid outflow, selecting robust hydrophilic materials, and maintaining device reusability after integration with a sodium sensor.
2. The fabricated microfluidic device must be tested to identify and address limitations related to design criteria such as dimensions, shape, and materials to ensure effective fluid flow and accurate sweat sodium measurements.
3. The wearable potentiostat should interface with a smartphone to provide an alternative to computers or laptops, allowing for wireless sweat sodium monitoring anywhere and being convenient to carry in a pocket. However, the smartphone app needs to be able to set input parameters, transmit data, display graphs, and save information to the cloud drive for the system to work properly.